energies

MDPI

*Article*

# Improved Method for Determining Voltage Unbalance Factor Using Induction Motors

**Luis Guasch-Pesquer [1,*], Sara García-Ríos [2], Adolfo Andres Jaramillo-Matta [3] and Enric Vidal-Idiarte [1]**

1 Department of Electronic, Electric and Automatic Engineering, Universitat Rovira i Virgili, Països Catalans, 26, 43007 Tarragona, Spain
2 IDNEO Technologies, S.A.U. Carrer Rec de Dalt 3, 08100 Mollet del Vallès, Spain
3 Facultad de Ingeniería, Universidad Distrital Francisco José de Caldas, Carrera 7 # 40B–53, Bogotá 111711, Colombia
* Correspondence: luis.guasch@urv.cat

**Abstract:** This work shows an alternative method to determine the Voltage Unbalance Factor in a power grid by using both the mean value of the line voltages and Current Unbalance Factor in induction motors. Twenty unbalanced voltage points on three induction motors were used in order to compare the two methods. The influence of the measurement error of both the voltmeters and the ammeters on the resulting Voltage Unbalance Factor was studied, and the validation was made with laboratory data for one of the three motors analyzed, in addition to the simulations carried out. The proposed Voltage Unbalance Factor was compared with the most typical method in the standards to obtain this factor, showing that the proposed factor has a better approach than the standard factor to determine the value of the Voltage Unbalance Factor in an unbalanced power system.

**Keywords:** current measurement; induction motors; power quality; torque measurement; voltage fluctuations

check for updates

**Citation:** Guasch-Pesquer, L.; García-Ríos, S.; Jaramillo-Matta, A.A.; Vidal-Idiarte, E. Improved Method for Determining Voltage Unbalance Factor Using Induction Motors. *Energies* **2022**, *15*, 9232. https://doi.org/10.3390/en15239232

Academic Editors: Agusti Egea-Alvarez, Lluís Monjo and Luis Sainz Sapera

Received: 10 October 2022
Accepted: 4 December 2022
Published: 6 December 2022



## 1. Introduction

Voltage unbalances are disturbances in three-phase electrical systems, which can be present for long periods of time and are regulated in many countries. Most of these standards use the Voltage Unbalance Factor (*VUF*) to quantify voltage unbalances, by determining appropriate values for an electrical network.

In practice, the correct measurement of the voltage unbalance factor (*VUF*) is necessary in measurement and control systems such as [1], where, due to the large variations in the power absorbed by trains, it is not possible to adequately limit the unbalance in the three-phase voltages with which, in order to correctly determine the unbalance of the system, it is necessary to accurately calculate the voltage unbalance factor based on the power consumed by the trains, or [2] where the inaccuracy of the formulas that make them unusable when an unbalanced system is connected has been taken into account because they do not consider the active and reactive powers separately. In [3], how to quantify voltage unbalances according to the standards is discussed, and a new methodology is proposed to quantify the voltage unbalance factor (*VUF*) by measuring the voltage unbalance in three-phase installations by means of a new intelligent sensor based on a unique voltage sensor, which measures the voltage in direct current (DC).

In this sense, in [4] it is indicated that the limit to consider a voltage system as balanced three-phase is *VUF* = 2%. Among the most relevant investigations in this field are those related to methods of compensating for voltage imbalances in the low-voltage networks of domestic consumers, produced mainly by the connection of single-phase devices in three-phase networks such as photovoltaic installations, batteries, and electric vehicle chargers, among others [5–9]. Another field of study is the determination of the location where imbalances are generated in a three-phase electrical network [10]. However, among the most outstanding studies are the effects produced by voltage unbalances in different types of loads, particularly in three-phase induction motors. In this field, the effects have been analyzed on: performance [11–15], torque [14,16,17], vibrations [16,18], current [17,18], temperature [15,19], power [16], power factor [15], noise [18] or performance types [20], as well as studies that analyze the influence of the power of the loads that generate unbalances in the *VUF* [21].

A final field of study to highlight is the characterization of voltage unbalances. In [13], the *VUF* (or other equivalents) and the typology are characterized by two parameters, defining eight different types of *VUF*. In [17], they are characterized by the *VUF*, the typology, and the direct component of the triphasic voltage, $V_1$. In [22], they are characterized by the *VUF* and the Equivalent Voltage Magnitude Factor.

Traditional methods for calculating the *VUF* ($VUF_1$) are based on measuring the RMS line voltages. In this work, an alternative method is proposed to calculate the *VUF* ($VUF_2$) from two parameters, the mean value of line voltages and the *Current Unbalance Factor* (*CUF*), obtained from the RMS line currents (in this case, the currents of an induction motor). As a result, the proposed method generates lower errors in the *VUF* calculation than the traditional methods, mainly when the power system presents values around *VUF* = 2%.

The proposed method to determine the *Voltage Unbalance Factor* ($VUF_2$) can be applied to determine the unbalance of an electrical network that feeds, among other loads, a three-phase induction motor.

## 2. Materials and Methods

### *2.1. Unbalance Factors in Three-Phase Electrical Systems*

This section defines the *VUF*, the current unbalance factor (*CUF*), and the mean value of a three-phase voltage system ($V_{\text{mean}}$).

#### 2.1.1. Voltage Unbalance Factor (VUF)

For an unbalanced three-phase voltage system, the *VUF* can be calculated with the mathematical expression (1), where $V_2$ is the module of the inverse component of the voltage, $V_1$ is the module of the direct component of the voltage, a = $0.5 \cdot (-1 + \text{j}\cdot\sqrt{3})$, and $\boldsymbol{V}_{\text{AB}}$, $\boldsymbol{V}_{\text{BC}}$, and $\boldsymbol{V}_{\text{CA}}$ are the line voltages of the system.

$$VUF(\%) = \frac{V_2}{V_1} \cdot 100 = \frac{\left|\frac{1}{3}\cdot\left(\boldsymbol{V}_{\text{AB}} + \text{a}^2\cdot\boldsymbol{V}_{\text{BC}} + \text{a}\cdot\boldsymbol{V}_{\text{CA}}\right)\right|}{\left|\frac{1}{3}\cdot\left(\boldsymbol{V}_{\text{AB}} + \text{a}\cdot\boldsymbol{V}_{\text{BC}} + \text{a}^2\cdot\boldsymbol{V}_{\text{CA}}\right)\right|} \tag{1}$$

#### 2.1.2. Current Unbalance Factor (CUF)

Similarly, the *CUF* can be calculated from (2). In this mathematical expression, $I_2$ is the module of the inverse component of the current, $I_1$ is the module of the direct component of the current, and $\boldsymbol{I}_{\text{A}}$, $\boldsymbol{I}_{\text{B}}$, and $\boldsymbol{I}_{\text{C}}$ are the line currents of the system.

$$CUF(\%) = \frac{I_2}{I_1} \cdot 100 = \frac{\left|\frac{1}{3}\cdot\left(\boldsymbol{I}_{\text{A}} + \text{a}^2\cdot\boldsymbol{I}_{\text{B}} + \text{a}\cdot\boldsymbol{I}_{\text{C}}\right)\right|}{\left|\frac{1}{3}\cdot\left(\boldsymbol{I}_{\text{A}} + \text{a}\cdot\boldsymbol{I}_{\text{B}} + \text{a}^2\cdot\boldsymbol{I}_{\text{C}}\right)\right|} \tag{2}$$

#### 2.1.3. Mean Voltage ($V_{\text{mean}}$)

The average value of the voltages (3), in a three-phase system, is a magnitude to be taken into account in the analysis of unbalances. In this mathematical expression, $V_{\text{AB}}$, $V_{\text{BC}}$, and $V_{\text{CA}}$ are the modules of the line voltages of the system.

$$V_{\text{mean}} = \frac{1}{3}\cdot\left(V_{\text{AB}} + V_{\text{BC}} + V_{\text{CA}}\right) \tag{3}$$

### 2.2. Voltage Unbalance Points

In this work, 20 voltage unbalance points were considered with 5 reference values for *VUF* (1, 2, 3, 4, and 5%) and 4 reference values for $V_{mean}$ (0.85, 0.90, 0.95, and 1.00 pu). From these values, the values of the modules and the angles of the line voltages are determined under the following criteria: no unbalance in the angles is considered; $V_{BC}$ is taken equal to $V_{mean}$; $V_{AB}$ and $V_{CA}$ are two equidistant values with respect to $V_{BC}$, the first lower and the second higher, which determine the *VUF* and $V_{mean}$ reference values chosen at each unbalance point.

The mathematical notation of the voltages at each unbalance point is shown in (4) and the values of $VUF_{ref}$, $V_{mean,ref}$, $V_{AB}$, $V_{BC}$, $V_{CA}$, $\varphi_{AB}$, $\varphi_{BA}$, and $\varphi_{CA}$ for the 20 selected unbalance points are shown in Table 1.

$$\mathbf{V}_{AB} = V_{AB}\ 0^\circ \quad ; \quad \mathbf{V}_{BC} = V_{BC}\ -120^\circ \quad ; \quad \mathbf{V}_{CA} = V_{CA}\ 120^\circ \tag{4}$$

**Table 1.** Setpoint values for 20 experimental unbalance points.

| Point | $VUF_{ref}$ (%) | $V_{mean,ref}$ (pu) | $V_{AB}$ (pu) | $V_{BC}$ (pu) | $V_{CA}$ (pu) | $\varphi_{AB}$ (°) | $\varphi_{BC}$ (°) | $\varphi_{CA}$ (°) |
|---|---|---|---|---|---|---|---|---|
| 1 | 1 | 0.85 | 0.835 | 0.850 | 0.865 | 0 | −120 | 120 |
| 2 | 1 | 0.90 | 0.884 | 0.900 | 0.916 | 0 | −120 | 120 |
| 3 | 1 | 0.95 | 0.934 | 0.950 | 0.966 | 0 | −120 | 120 |
| 4 | 1 | 1.00 | 0.983 | 1.000 | 1.017 | 0 | −120 | 120 |
| 5 | 2 | 0.85 | 0.821 | 0.850 | 0.879 | 0 | −120 | 120 |
| 6 | 2 | 0.90 | 0.869 | 0.900 | 0.931 | 0 | −120 | 120 |
| 7 | 2 | 0.95 | 0.917 | 0.950 | 0.983 | 0 | −120 | 120 |
| 8 | 2 | 1.00 | 0.965 | 1.000 | 1.035 | 0 | −120 | 120 |
| 9 | 3 | 0.85 | 0.806 | 0.850 | 0.894 | 0 | −120 | 120 |
| 10 | 3 | 0.90 | 0.853 | 0.900 | 0.947 | 0 | −120 | 120 |
| 11 | 3 | 0.95 | 0.901 | 0.950 | 0.999 | 0 | −120 | 120 |
| 12 | 3 | 1.00 | 0.948 | 1.000 | 1.052 | 0 | −120 | 120 |
| 13 | 4 | 0.85 | 0.791 | 0.850 | 0.909 | 0 | −120 | 120 |
| 14 | 4 | 0.90 | 0.838 | 0.900 | 0.962 | 0 | −120 | 120 |
| 15 | 4 | 0.95 | 0.884 | 0.950 | 1.016 | 0 | −120 | 120 |
| 16 | 4 | 1.00 | 0.931 | 1.000 | 1.069 | 0 | −120 | 120 |
| 17 | 5 | 0.85 | 0.776 | 0.850 | 0.924 | 0 | −120 | 120 |
| 18 | 5 | 0.90 | 0.822 | 0.900 | 0.978 | 0 | −120 | 120 |
| 19 | 5 | 0.95 | 0.868 | 0.950 | 1.032 | 0 | −120 | 120 |
| 20 | 5 | 1.00 | 0.913 | 1.000 | 1.087 | 0 | −120 | 120 |

### 2.3. Measuring Instruments

The measurement error in the RMS values of voltage and current determine errors in the calculation of *VUF* and *CUF*. The influence of these errors is much greater in the case of *VUF*. For this reason, in this work a new method for the determination of *VUF* is proposed.

Although the values of power, voltage, and current at the nominal operating point are different in the three motors analyzed in this work, in order to simplify the calculations, the measuring errors on only one instrument were taken as reference, the Fluke 87V industrial multimeter. This instrument has an accuracy of ±(0.7% + 2) in the RMS voltage measurement and ±(1.0% + 2) in the RMS current measurement.

The error in the measurement of the RMS value of the voltage, for a real RMS value of 100 V, implies that the readings can oscillate between a minimum value of 99.1 V and a maximum value of 100.9 V. The error in the measurement of the value current, for a real value of 10 A, implies that the readings can oscillate between a minimum value of 9.88 A and a maximum value of 10.12 A.

Figure 1 shows the waveform of the 230 V line voltages for Point 2 in Table 1, with $VUF_{ref}$ = 1% and $V_{mean,ref}$ = 0.90.

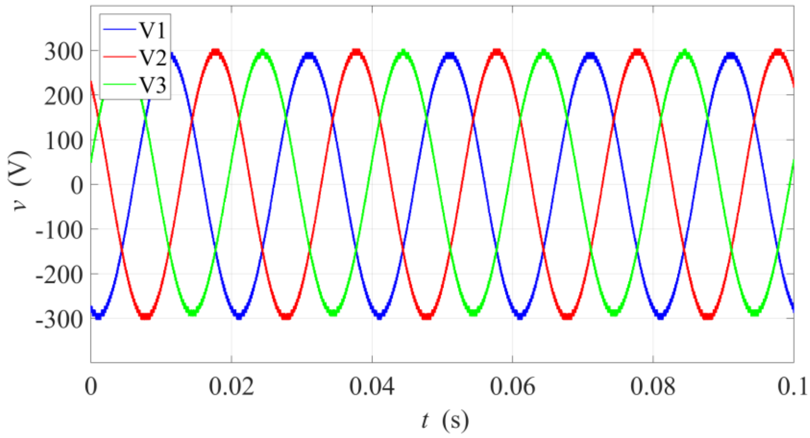


**Figure 1.** Three-line unbalance voltages for Point 2 in Table 1, with $VUF_{ref}$ = 1% and $V_{mean,ref}$ = 0.90.

### 2.4. Induction Motors

In this work, the effect of voltage unbalances in three induction motors has been analyzed: Motor A (1.5 kW), Motor B (7.5 kW), and Motor C (75 kW). The analysis was carried out through tests in the laboratory for Motor A and through simulations for the three motors.

#### 2.4.1. Induction Motors Characteristics

Table 2 shows the characteristics of the 3 motors selected for this work at the rated operating point. Motors with different characteristics were chosen in order to see if the results obtained are similar in all cases.

**Table 2.** Characteristics of induction motors at the rated operating point.

| Rated Point | Motor A | Motor B | Motor C |
|---|---|---|---|
| Power (kW) | 1.5 | 7.5 | 75.0 |
| Voltage (V) | 230 | 400 | 3300 |
| Frequency (Hz) | 50 | 50 | 50 |
| Connection | Delta | Star | Star |
| Current (A) | 6.00 | 15.3 | 15.3 |
| Speed ($min^{-1}$) | 1420 | 1460 | 1455 |
| Torque (Nm) | 10.1 | 49.0 | 492.2 |

#### 2.4.2. Mathematical Model

In order to simulate the performance of induction motors under voltage unbalance, the single-cage model with five constant parameters was selected. This model can be represented by the equivalent circuit shown in Figure 2, where $R_s$ and $R_r$ are the stator and rotor resistances, respectively; $X_m$ is the magnetizing reactance; $X_{sd}$ and $X_{rd}$ are the stator and rotor reactances, and *s* is the slip.

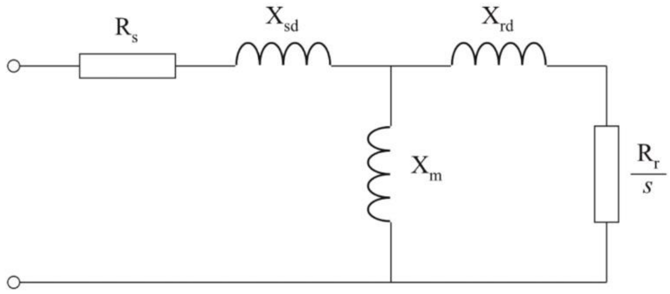


**Figure 2.** Equivalent circuit with five constant parameters for the single-cage model of the induction motor.

### 2.4.3. Parameters

Table 3 shows the electrical parameters of the three motors analyzed.

**Table 3.** Electrical parameters of the induction motors.

| Parameter | Motor A | Motor B | Motor C |
|---|---|---|---|
| $R_s$ (Ω) | 3.72 | 0.85 | 7.52 |
| $R_r$ (Ω) | 4.50 | 0.57 | 3.51 |
| $X_m$ (Ω) | 107.73 | 27.5 | 577.3 |
| $X_{sd}$ (Ω) | 7.99 | 1.37 | 12.6 |
| $X_{rd}$ (Ω) | 7.99 | 1.37 | 12.6 |

## *2.5. Laboratory Setup and Methodology*

Motor A was tested in the laboratory, at the 20 unbalance points indicated in Table 1. In each test, the motor was made to reach the rated operating point by means of a programmable voltage source (Figure 3), which was configured to apply the voltages corresponding to the unbalance point. As a mechanical load, a direct current generator was used, which fed a resistive load (Figure 3). With the motor in unbalanced conditions, the following were recorded for one second: line voltages and currents, speed, and torque. From the temporal evolution of the currents, it was possible to obtain the *CUF* caused by the voltage unbalance.

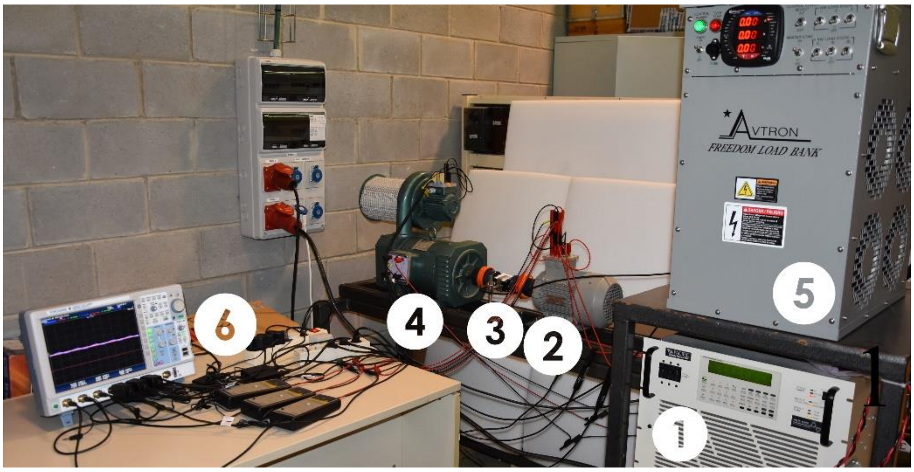


**Figure 3.** General overview of laboratory setup used in the tests. The main devices are: (1) programmable power source; (2) induction motor; (3) torque and speed sensors; (4) DC generator; (5) DC generator's resistive load; (6) oscilloscope.

## 3. Results

The results are presented in five sections. First, the evolution of the *CUF* with respect to the *VUF* is shown, for the experimental and simulation results of Motor A, with constant $V_{mean}$.

Then, the influence of the measurement error in the voltmeters for the calculation of the *VUF* and the influence of the measurement error in the ammeters for the calculation of the *CUF* in the three analyzed motors are calculated.

Thirdly, the proposed method for calculating the *VUF* based on $V_{mean}$ and *CUF* for the three motors analyzed is presented, assuming that there are no errors in the measurement instruments.

Fourth, the *VUF* values are calculated as a function of $V_{mean}$ and *CUF*, taking into account the maximum possible error in $V_{mean}$ (generated by the error in the three voltmeters) and the maximum error in *CUF* (generated by the error in the three ammeters).

Finally, the errors are compared when calculating the *VUF* directly from the three voltmeters vs. the errors when calculating the *VUF* from *CUF* and $V_{mean}$.

### 3.1. CUF vs. VUF Ratio

In [16] it was already shown that there is a practically linear ratio between the values of the *VUF* and the *CUF*, when the same value of the direct component of unbalanced voltage ($V_1$) is chosen. In that work, all the results were obtained from the simulation of 13,060 unbalance points for motors B and C.

In this work, Motor A was added, for which the ratio between *VUF* and *CUF* was studied, based on the experimental and simulation results in the 20 unbalance points defined in the previous section.

The results are shown in Figure 4, through 4 graphs: (a) $V_{mean}$ = 0.85 pu; (b) $V_{mean}$ = 0.90 pu; (c) $V_{mean}$ = 0.95 pu; (d) $V_{mean}$ = 1.00 pu. In each graph, the experimental results are shown by means of a blue line, and the simulation results by means of a cyan line. In the four cases, it is observed that the experimental and simulation results are close, but this assessment is quantified later in the discussion section.

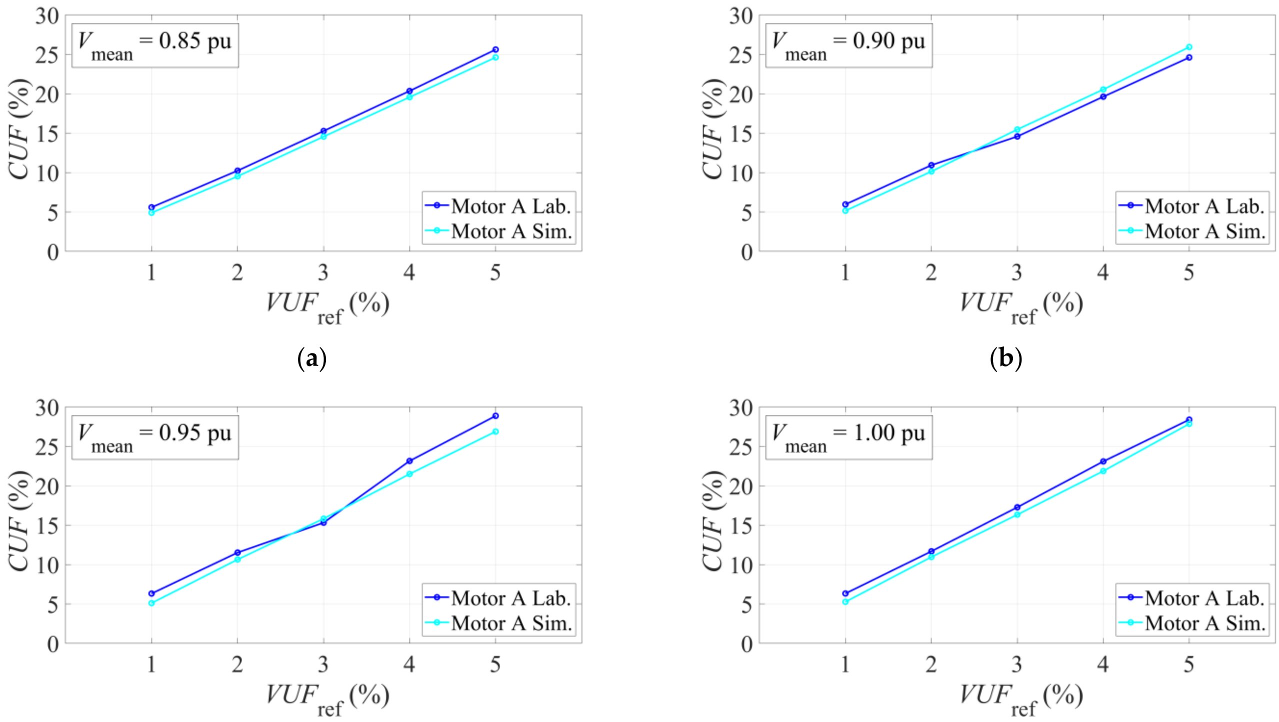


(**a**) (**b**) (**c**) (**d**)

**Figure 4.** *CUF* vs. *VUF* on motor A for experimental (blue) and simulation (cyan) results, and different values of $V_{mean}$: (**a**) 0.85 pu; (**b**) 0.90 pu; (**c**) 0.95 pu; (**d**) 1.00 pu.

In all the graphs of Figure 4, a practically linear ratio between the values of *VUF* and *CUF* is observed, for $V_{mean}$ constant.

### 3.2. Impact of Measurement Errors on the VUF and CUF

In this section, the voltage ($VUF_{0.7}$) and current ($CUF_{1.0}$) unbalance factors are calculated, when the maximum measurement error in the selected instrument is taken into account, for the 20 unbalance points previously defined.

In the case of voltage, the RMS value of the minimum voltage ($V_{AB}$) was multiplied by 0.991, and the RMS value of the maximum voltage ($\mathbf{V}_{CA}$) by 1.009, leaving $V_{BC}$ unchanged, as shown in (5).

$$V_{AB,0.7} = 0.991 \cdot V_{AB} \quad ; \quad V_{BC,0.7} = V_{BC} \quad ; \quad V_{CA,0.7} = 1.009 \cdot V_{CA} \tag{5}$$

From the new RMS voltage values ($\boldsymbol{V}_{AB,0.7}$, $\boldsymbol{V}_{BC,0.7}$, and $\boldsymbol{V}_{CA,0.7}$), the new voltage unbalance factor $VUF_1$ was calculated at each of the 20 points according to (6).

$$VUF_1(\%) = \frac{V_{2,0.7}}{V_{1,0.7}} \cdot 100 = \frac{\left| \frac{1}{3} \cdot \left( \boldsymbol{V}_{AB,0.7} + \mathrm{a}^2 \cdot \boldsymbol{V}_{BC,0.7} + \mathrm{a} \cdot \boldsymbol{V}_{CA,0.7} \right) \right|}{\left| \frac{1}{3} \cdot \left( \boldsymbol{V}_{AB,0.7} + \mathrm{a} \cdot \boldsymbol{V}_{BC,0.7} + \mathrm{a}^2 \cdot \boldsymbol{V}_{CA,0.7} \right) \right|} \quad (6)$$

This new unbalance value was also compared with the reference value using $e_{VUF1}$, as shown in (7).

$$e_{VUF1}(\%) = \frac{VUF_{0.7} - VUF_{ref}}{VUF_{ref}} \cdot 100 \quad (7)$$

Applying (7) to all the unbalance points, Figure 5a shows the $e_{VUF1}$ values by means of isolines. The vertical axis corresponds to the reference VUF ($VUF_{ref}$), and the horizontal axis to the mean value of the line voltages ($V_{mean}$). Right at the value where many standards mark the unbalance limit, $VUF_{ref}$ = 2%, it is observed that the error in the calculation of the *VUF* through (6), when the measurement error in the effective value of the voltage is 0.7% ($e_v$ = 0.7%), can give rise to errors of 30% in the VUF ($e_{VUF1=2\%} \approx 30\%$).

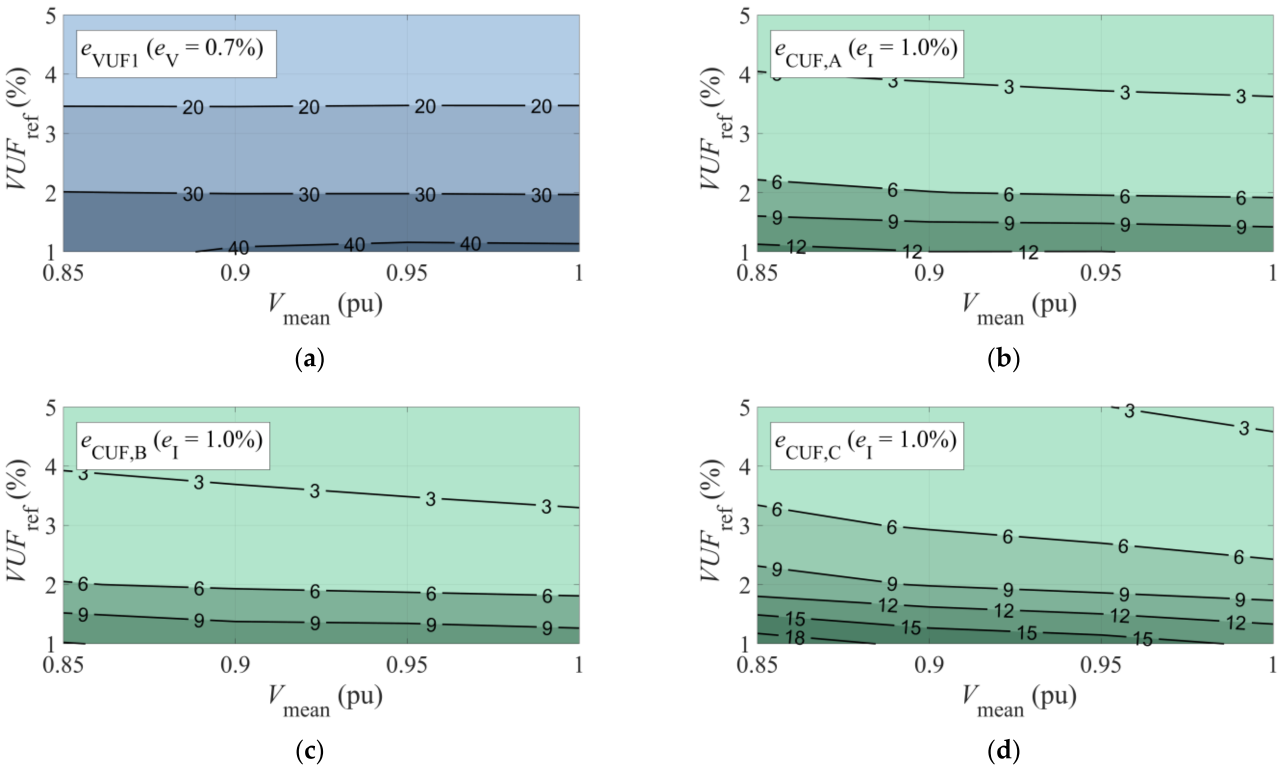


**Figure 5.** (**a**) *VUF* error ($e_{VUF1}$) according to $V_{mean}$ and $VUF_{ref}$ when the measurement error in the voltmeters is 0.7%; *CUF* error ($e_{CUF}$) according to $V_{mean}$ and $VUF_{ref}$ when the measurement error in the ammeters is 1.0%: (**b**) Motor A; (**c**) Motor B; (**d**) Motor C.

For the current unbalance calculation, the precision in the measurement of the rated value of the current by means of the Fluke 87V industrial multimeter was also taken into account. To obtain the most unfavorable case, the minimum current RMS value of the three phases was multiplied by 0.988, and the maximum current RMS value of the three phases by 1.012, leaving the remaining phase unchanged, which is the median of the three values RMS of current (8).

$$I_{min} = 0.988 \cdot \min\{I_A, I_B, I_C\} \;;\; I_{max} = 1.012 \cdot \max\{I_A, I_B, I_C\}$$
$$I_{median} = \mathrm{median}\{I_A, I_B, I_C\} \quad (8)$$

Regarding the angles of the line currents, both in the experimental results and in the simulation results of the 20 unbalanced points analyzed, it was observed that the phase shift of the currents is not 120°. However, in this work, no error in the measurement of the angles was considered. The new current phasors are defined in (9).

$$\boldsymbol{I}_{\min} = I_{\min}\ \varphi_{\min} \quad ; \quad \boldsymbol{I}_{\mathrm{median}} = I_{\mathrm{median}}\ \varphi_{\mathrm{median}} \quad ; \quad \boldsymbol{I}_{\max} = I_{\max}\ \varphi_{\max} \tag{9}$$

From the new current values, the new current unbalance $CUF_{1.0}$ (10) was calculated.

$$CUF_{1.0}(\%) = \frac{I_{2,1.0}}{I_{1,1.0}} \cdot 100 = \frac{\left|\frac{1}{3}\cdot\left(\boldsymbol{I}_{\min} + \mathrm{a}^2\cdot\boldsymbol{I}_{\mathrm{median}} + \mathrm{a}\cdot\boldsymbol{I}_{\max}\right)\right|}{\left|\frac{1}{3}\cdot\left(\boldsymbol{I}_{\min} + \mathrm{a}\cdot\boldsymbol{I}_{\mathrm{median}} + \mathrm{a}^2\cdot\boldsymbol{I}_{\max}\right)\right|} \tag{10}$$

Finally, for a given unbalanced point and motor, the error in the *CUF*, $e_{\mathrm{CUF}}$, can be calculated by using (11).

$$e_{\mathrm{CUF}}(\%) = \frac{CUF_{1.0} - CUF_{\mathrm{ref}}}{CUF_{\mathrm{ref}}} \cdot 100 \tag{11}$$

Figure 5b–d shows the *CUF* errors for motors A, B, and C, as a function of $V_{\mathrm{mean}}$ and $VUF_{\mathrm{ref}}$. As can be seen, despite the fact that the error in the ammeters is greater (1%) than in the voltmeters (0.7%), $e_{\mathrm{CUF}}$ is less than $e_{\mathrm{VUF}}$ for all values of $VUF_{\mathrm{ref}}$ because the *CUF* is much greater than the *VUF* that originates it, in all engines, and for all operating points. Observing the simulation results of the three motors, for a value $VUF_{\mathrm{ref}}$ = 2%, $e_{\mathrm{CUF}}$ is approximately between 6% and 11%. These values are clearly lower than the errors observed in $e_{\mathrm{VUF}}$ for the same reference value, which are around 30% ($e_{\mathrm{VUF=2\%}} \approx 30\%$).

### *3.3. Proposed Method for VUF Calculation (Method 2—$VUF_2$)*

Figure 6 shows the *VUF* value as a function of $V_{\mathrm{mean}}$ and *CUF* by using isolines: (a) laboratory results for motor A; (b) simulation results for motor A; (c) simulation results for motor B; (d) simulation results for motor C.

Using the corresponding graph in Figure 6 (depending on the motor used and whether the starting data are from the laboratory or simulation), the value of $VUF_2$ can be determined from the values of $V_{\mathrm{mean}}$ and *CUF* (12).

$$VUF_2 = VUF(V_{\mathrm{mean}}, CUF_{\mathrm{ref}}) \tag{12}$$

### *3.4. Influence of Measurement Errors on $VUF_2$*

In this section, only the simulation results for the three motors are taken: A, B, and C.

At each of the 20 unbalance points, the maximum error in the *VUF*, $e_{\mathrm{VUF2,max}}$, is calculated when it is obtained from $V_{\mathrm{mean}}$ and *CUF*. For this, the maximum error in $V_{\mathrm{mean}}$ due to the voltmeters and the maximum error in the *CUF* due to the ammeters are considered.

As an example, Figure 7 shows that with values of $V_{\mathrm{mean}}$ = 0.95 pu and *CUF* = 15%, a *VUF* of 2.58% is obtained ($VUF_{0.95,15}$ = 2.58%). If the maximum error of the voltmeters is taken into account to calculate $V_{\mathrm{mean}}$, when it is 0.95 pu, it implies an oscillation of ±0.09; therefore, $V_{\mathrm{mean,min}}$ = 0.941 and $V_{\mathrm{mean,\,max}}$ = 0.959. Similarly, if the maximum error of the ammeters is taken into account to calculate the *CUF*, when it is 15%, it implies an oscillation of 0.7%; therefore, $CUF_{\min}$ = 14.3% and $CUF_{\max}$ = 15.7%. These tolerances give rise to a rectangular surface, where the four vertices, *k* = {I, II, III and IV}, are the points farthest from the central reference point. The value of $VUF_{k,m}$ is obtained from $V_{\mathrm{mean}}$ and *CUF* in these four vertices for each motor, where *m* refers to the test motors, *m* = {A, B and C}, and the $e_{\mathrm{VUF},k,m}$ is calculated in each of them, according to expression (13). Finally, the $e_{\mathrm{VUF},2}$ for the coordinate ($V_{\mathrm{mean}}$, *CUF*) will be the largest of those calculated at the vertices, as shown in (14). As can be seen, with the parameters in Figure 7, measurement errors can generate *VUF* values between 2.45% and 2.72%.

$$e_{\mathrm{VUF2},k,M}(\%) = \frac{VUF_{k,m} - VUF_{\mathrm{ref}}}{VUF_{\mathrm{ref}}} \cdot 100 \quad k = \{\mathrm{I, II, III, IV}\} \;\; ; \;\; M = \{\mathrm{A,\ B,\ C}\} \tag{13}$$

$$e_{\mathrm{VUF2},M}(\%) = \max\{e_{\mathrm{VUF2},k,M}\} \tag{14}$$

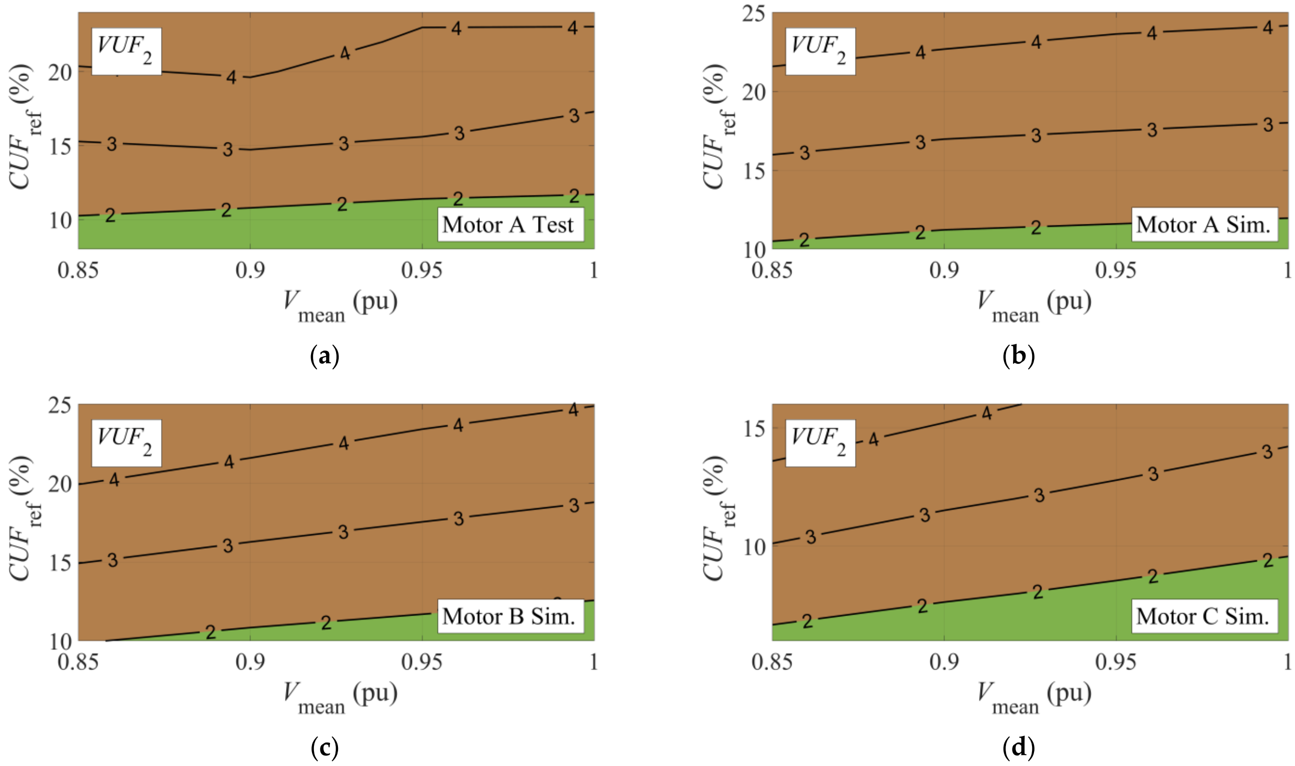


**Figure 6.** $VUF_2$ according to $V_{\mathrm{mean}}$ and $CUF$ for: (**a**) Test results for Motor A; (**b**) Simulation results for Motor A; (**c**) Simulation results for Motor B; (**d**) Simulation results for Motor C.

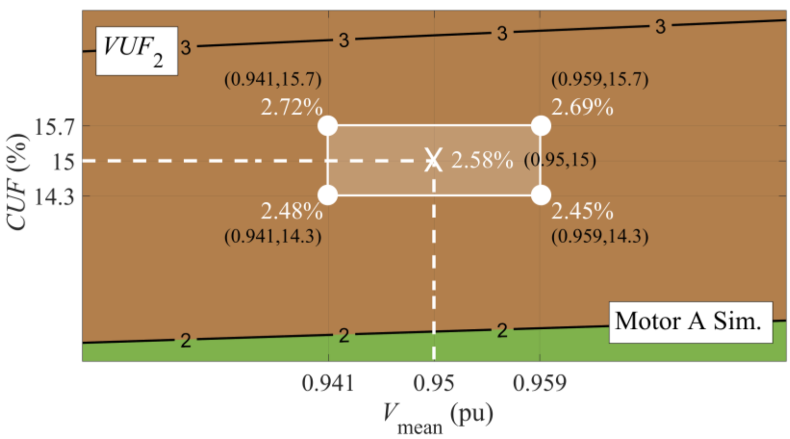


**Figure 7.** $VUF_2$ according to measurement errors.

### 3.5. Comparison of Methods to Obtain VUF

Finally, the errors in the *VUF* calculation are compared, when it is calculated from the effective value of the three voltmeters -Method 1-, $e_{\mathrm{VUF},1}$ (Figure 8a), or when it is calculated from $V_{\mathrm{mean}}$ and *CUF* in each of the three motors analyzed -Method 2-: $e_{\mathrm{VUF2,A}}$ (Figure 8b), $e_{\mathrm{VUF2,B}}$ (Figure 8c), and $e_{\mathrm{VUF2,C}}$ (Figure 8d).

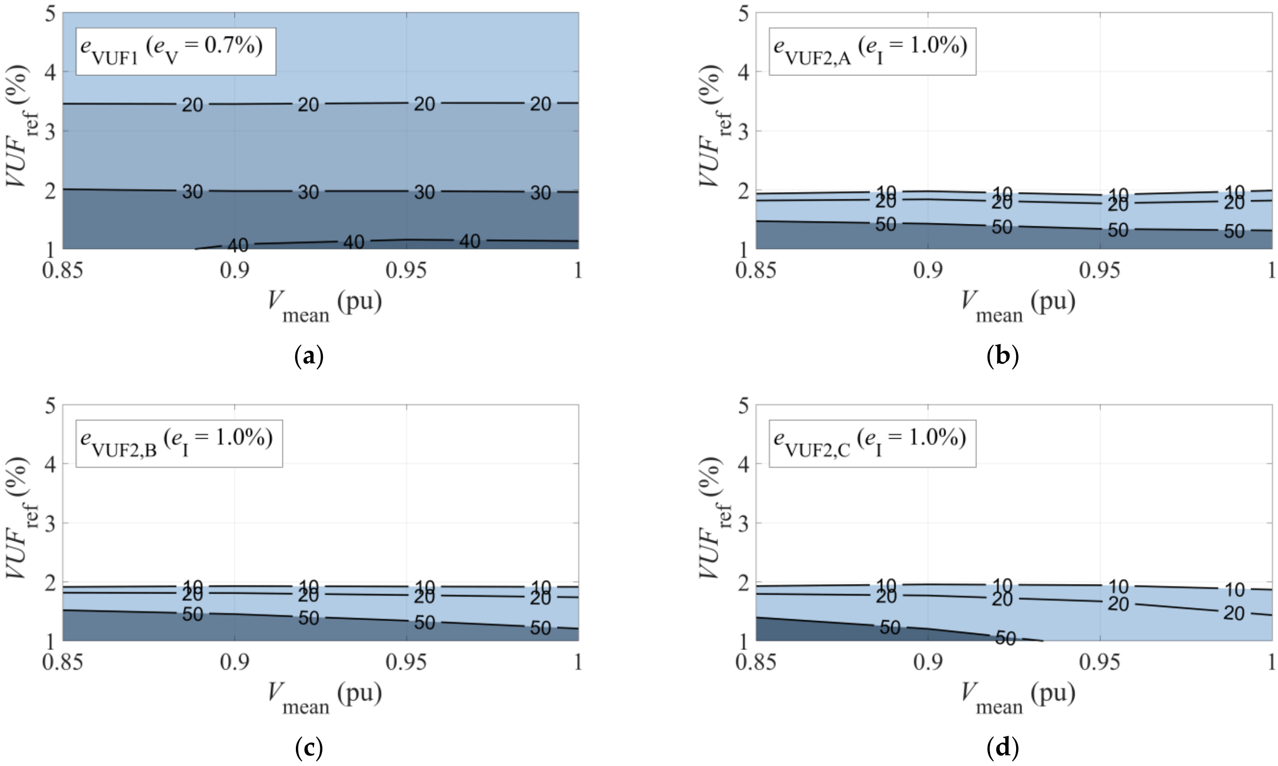


**Figure 8.** *VUF* error according to *VUF* and $V_{\text{mean}}$: (**a**) for Motor A, obtained from $e_{\text{VUF,1}}$; (**b**) for Motor A, obtained from $e_{\text{VUF2,A}}$; (**c**) for Motor B, obtained from $e_{\text{VUF2,B}}$; (**d**) for Motor C, obtained from $e_{\text{VUF2,C}}$.

If all the graphs in Figure 8 are compared for $VUF_{\text{ref}}$ = 2%, it is observed that $e_{\text{VUF1}} \approx$ 30%, while $e_{\text{VUF,2,A}}$, $e_{\text{VUF,2,B}}$, and $e_{\text{VUF,2,C}}$ are less than 10%.

## 4. Discussion

This section analyzes the results obtained in the previous section.

### *4.1. Ratio between CUF and VUF*

In order to quantify the error between the *CUF* values in Motor A, obtained from experimental results (blue lines in Figure 4) and simulation results (cyan lines in Figure 4), the mean square error was calculated in the 20 points of unbalance through (15), obtaining 1.03% as a result.

$$e_{\text{CUF,A}}(\%) = \sqrt{\frac{\sum_{n=1}^{n=20} (CUF_{\text{sim}} - CUF_{\text{test}})^2}{N}} = 1.03\% \tag{15}$$

It is considered that this error corroborates the proximity observed in the previous section between the laboratory and simulation results obtained for Motor A.

### *4.2. Influence of Measurement Errors on the VUF and CUF*

This section presents and analyzes the results of $e_{\text{VUF1}}$, $e_{\text{CUF,A}}$, $e_{\text{CUF,B}}$, and $e_{\text{CUF,C}}$, when $VUF_{\text{ref}}$ = 2%. The numerical results are presented in Table 4.

**Table 4.** *VUF* and *CUF* errors for $VUF_{\text{ref}}$ = 2%.

| $e_{\text{VUF1}}$ (%) | $e_{\text{CUF,A}}$ (%) | $e_{\text{CUF,B}}$ (%) | $e_{\text{CUF,C}}$ (%) |
|---|---|---|---|
| 29.8 | 5.9 | 5.5 | 8.4 |

These results show that the *VUF* calculation, from the RMS voltage of voltmeters, gives rise to an error of 29.8%, when $VUF_{ref}$ = 2%. This fact determines a very high probability of error in determining the balance of the voltage supply provided by an electric company to a customer.

The results also show that in the *CUF* calculation, from the RMS current in the ammeters, the error is notably lower than that observed in the *VUF*, when $VUF_{ref}$ = 2%. The *CUF* error is smaller because the current unbalances in three-phase induction motors are considerably higher than the voltage unbalances that originate them.

### 4.3. *VUF as Function of $V_{mean}$ and CUF*

Figure 6a,b shows the *VUF* values from the laboratory and simulation results for Motor A.

Table 5 shows the $VUF_2$ values, obtained from $V_{mean}$ and $CUF_{ref}$ coordinates, when data come from the laboratory for Motor A, for $VUF_{ref} \approx 2\%$. Similarly, Table 6 shows the values of $VUF_2$, for the same coordinates $V_{mean}$ and $CUF_{ref}$, from simulation results ($VUF_{ref} \approx 2\%$). The results are quite close to the reference value, being higher when the unbalance is greater.

**Table 5.** $VUF_2$ from $V_{mean}$ and $CUF_{ref}$, from the laboratory tests of Motor A.

| | $VUF_2$ (%) | | | |
|---|---|---|---|---|
| | $V_{mean}$ = 0.85 | $V_{mean}$ = 0.90 | $V_{mean}$ = 0.95 | $V_{mean}$ = 1.00 |
| $CUF_{ref}$ = 14% | 2.75 | 2.84 | 2.65 | 2.42 |
| $CUF_{ref}$ = 12% | 2.35 | 2.29 | 2.13 | 2.06 |
| $CUF_{ref}$ = 10% | 1.95 | 1.81 | 1.71 | 1.69 |

**Table 6.** $VUF_2$ from $V_{mean}$ and $CUF_{ref}$, from the simulation results of Motor A.

| | $VUF_2$ (%) | | | |
|---|---|---|---|---|
| | $V_{mean}$ = 0.85 | $V_{mean}$ = 0.90 | $V_{mean}$ = 0.95 | $V_{mean}$ = 1.00 |
| $CUF_{ref}$ = 14% | 2.64 | 2.48 | 2.41 | 2.34 |
| $CUF_{ref}$ = 12% | 2.27 | 2.13 | 2.07 | 2.01 |
| $CUF_{ref}$ = 10% | 1.91 | 1.79 | 1.73 | 1.68 |

Comparing the simulation results between the three motors (Figure 6a–c), similar behaviors are observed, but with different numerical values. For a constant *CUF* value, the *VUF* decreases roughly linear with increasing $V_{mean}$. For a constant $V_{mean}$ value, the *VUF* increases roughly linear with increasing *CUF*.

### 4.4. *Influence of Measurement Errors on $V_{mean}$ and CUF*

Table 7 shows the mean values of the errors in the *VUF*, for $VUF_{ref}$ = 2%, for methods 1 and 2.

**Table 7.** *VUF* errors for $VUF_{ref}$ = 2%.

| $e_{VUF,1}$ (%) | $e_{VUF,2,A}$ (%) | $e_{VUF,2,B}$ (%) | $e_{VUF,2,C}$ (%) |
|---|---|---|---|
| 29.8 | 6.5 | 4.0 | 7.1 |

Both the graphical results shown in Section 3.4, and the numerical ones in Table 7, show that obtaining the *VUF* value has less error if it is calculated from the average value of the three voltmeters and the *CUF* value (obtained from the three ammeters) than if calculated from the RMS voltage of the voltmeters. Method 2, proposed, is more accurate and appropriate to determine if an electrical energy supply can be considered balanced, or not, according to present regulations.

## 5. Conclusions

From the experimental results, it is confirmed that there is a roughly linear ratio between the *Current Unbalance Factor* and the *Voltage Unbalance Factor*, for a constant value of mean voltage supply lines.

The measurement errors in the voltmeters have a great influence on the calculation of the *Voltage Unbalance Factor*, particularly for 2%, the maximum value to consider a balanced system according to many standards.

For a three-phase induction motor powered by an unbalanced voltage system, measurement errors in the ammeters also affect the *Current Unbalance Factor* calculation, but to a lesser extent. This is because the current unbalances are greater than the voltage unbalances that cause them.

A new method for calculating the *Voltage Unbalance Factor* is proposed, based on the mean voltage supply lines that feed a three-phase induction motor, and the *Current Unbalance Factor* on the motor. This new method presents less error than the conventional one, where the mean values are obtained from the *Root Mean Square* value of the line voltages.

**Author Contributions:** Conceptualization, L.G.-P., S.G.-R., A.A.J.-M. and E.V.-I.; methodology, L.G.-P., S.G.-R., A.A.J.-M. and E.V.-I.; software, L.G.-P. and S.G.-R.; validation, L.G.-P., S.G.-R., A.A.J.-M. and E.V.-I.; formal analysis, L.G.-P., S.G.-R., A.A.J.-M. and E.V.-I.; investigation, L.G.-P., S.G.-R., A.A.J.-M. and E.V.-I.; resources, L.G.-P. and E.V.-I.; data curation, L.G.-P. and A.A.J.-M.; writing—original draft preparation, L.G.-P. and A.A.J.-M.; writing—review and editing, L.G.-P., S.G.-R., A.A.J.-M. and E.V.-I.; visualization, L.G.-P., S.G.-R., A.A.J.-M. and E.V.-I.; supervision, L.G.-P., S.G.-R., A.A.J.-M. and E.V.-I.; project administration, L.G.-P. and E.V.-I.; funding acquisition, E.V.-I. All authors have read and agreed to the published version of the manuscript.

**Funding:** Grant PID2021-124229NB-I00 funded by MCIN/AEI/10.13039/501100011033 and by "ERDF A way of making Europe".

**Conflicts of Interest:** The authors declare no conflict of interest.

## References

1. Flumian, D.; Ladoux, P.; Sarraute, E. Calculation of the Voltage Unbalance Factor for High-Speed Railway Substations with V-Connection Scheme. *Electronics* **2022**, *11*, 595. [CrossRef]
2. Flumian, D.; Ladoux, P.; Sarraute, E. Calculation of the Voltage Unbalance Factor for 25 kV–50 Hz Railway Substations. In Proceedings of the 2022 International Conference on Harmonics & Quality of Power, Naples, Italy, 29 May–1 June 2022.
3. Bogarra, S.; Saura, J.; Rolán, A. New Smart Sensor for Voltage Unbalance Measurements in Electrical Power Systems. *Sensors* **2022**, *22*, 8236. [CrossRef] [PubMed]
4. EN50160: 'Voltage Characteristics of Electricity Supplied by Public Electricity Net-Works'. Available online: https://www.en-standard.eu/21-30431799-dc-bs-en-50160-voltage-characteristics-of-electricity-supplied-by-public-distribution-networks/ (accessed on 1 July 2010).
5. Hamici, Z.; Abu-Elhaija, W. Power Conditioning with Intelligent Control Using a Novel Recursive Stochastic Optimization. *IEEE Trans. Ind. Electron.* **2019**, *66*, 3721–3730. [CrossRef]
6. Mousavi, S.Y.M.; Jalilian, A.; Savaghebi, M.; Guerrero, J.M. Flexible compensation of voltage and current unbalance and harmonics in microgrids. *Energies* **2017**, *10*, 1568. [CrossRef]
7. Nakadomari, A.; Shigenobu, R.; Kato, T.; Krishnan, N.; Hemeida, A.M.; Takahashi, H.; Senjyu, T. Unbalanced voltage compensation with optimal voltage controlled regulators and load ratio control transformer. *Energies* **2021**, *14*, 2997. [CrossRef]
8. Saroha, J.; Singh, M.; Jain, D.K. ANFIS-Based add-on controller for unbalance voltage compensation in a low-voltage microgrid. *IEEE Trans. Ind. Inform.* **2018**, *14*, 5338–5345. [CrossRef]
9. Shigenobu, R.; Nakadomari, A.; Hong, Y.Y.; Mandal, P.; Takahashi, H.; Senjyu, T. Optimization of voltage unbalance compensation by smart inverter. *Energies* **2020**, *13*, 4623. [CrossRef]
10. Pérez Vallés, A.; Salmerón Revuelta, P. A new distributed measurement index for the identification of harmonic distortion and/or unbalance sources based on the IEEE Std. 1459 framework. *Electr. Power Syst. Res.* **2019**, *172*, 96–104. [CrossRef]
11. Aderibigbe, A.; Ogunjuyigbe, A.; Ayodele, R.; Samuel, I. The performance of a 3-phase induction machine under unbalance voltage regime. *J. Eng. Sci. Technol. Rev.* **2017**, *10*, 136–143. [CrossRef]

12. Al-Badri, M.; Pillay, P.; Angers, P. A Novel in Situ Efficiency Estimation Algorithm for Three-Phase Induction Motors Operating with Distorted Unbalanced Voltages. *IEEE Trans. Ind. Appl.* **2017**, *53*, 5338–5347. [CrossRef]
13. Deleanu, S.; von Lipinski, G.; Iordache, M.; Stanculescu, M.; Niculae, D. Performance Evaluation of the Three-Phase Induction Motor Operating in Conditions of Unbalanced Voltage Supply. In Proceedings of the 8th International Conference on Modern Power Systems, Cluj-Napoca, Romania, 21–23 May 2019.
14. Fernandes Neves, A.B.; de Leles Ferreira Filho, A.; de Mendonça, M.V.B. Effects of voltage unbalance on torque and efficiency of a three-phase induction motor. In Proceedings of the International Conference on Harmonics and Quality of Power, Belo Horizonte, Brazil, 16–19 October 2016; pp. 679–683.
15. Lee, C.Y.; Chen, B.K.; Lee, W.J.; Hsu, Y.F. Effects of various unbalanced voltages on the operation performance of an induction motor under the same voltage unbalance factor condition. *Electr. Power Syst. Res.* **1998**, *47*, 153–163. [CrossRef]
16. Donolo, P.; Bossio, G.; de Angelo, C.; García, G.; Donolo, M. Voltage unbalance and harmonic distortion effects on induction motor power, torque and vibrations. *Electr. Power Syst. Res.* **2016**, *140*, 866–873. [CrossRef]
17. Guasch-Pesquer, L.; Jaramillo-Matta, A.A.; Gonzalez-Molina, F.; Garcia-Rios, S. Analysis of Current Unbalance and Torque Ripple Generated by Simulations of Voltage Unbalance in Induction Motors. In Proceedings of the Workshop on Engineering Applications, Cartagena, Colombia, 27–29 September 2017.
18. Mollet, Y.; Pergolesi, M.; Sarrazin, M.; Janssens, K.; van der Auweraer, H.; Chiariotti, P.; Castellini, P.; Gyselinck, J. Multi-Physical Signature Analysis of Induction Machines under Unbalanced Supply Voltage. In Proceedings of the International Conference on Electrical Machines, Alexandroupoli, Greece, 3–6 September 2018; pp. 2378–2384.
19. Gonzalez-Cordoba, J.L.; Osornio-Rios, R.A.; Granados-Lieberman, D.; Romero-Troncoso, R.D.J.; Valtierra-Rodriguez, M. Correlation Model between Voltage Unbalance and Mechanical Overload Based on Thermal Effect at the Induction Motor Stator. *IEEE Trans. Energy Convers.* **2017**, *32*, 1602–1610. [CrossRef]
20. Munoz Tabora, J.; de Lima Tostes, M.E.; Ortiz De Matos, E.; Holanda Bezerra, U.; Mota Soares, T.; Santana De Albuquerque, B. Assessing Voltage Unbalance Conditions in IE2, IE3 and IE4 Classes Induction Motors. *IEEE Access* **2020**, *8*, 186725–186739. [CrossRef]
21. Kim, Y.J. Development and Analysis of a Sensitivity Matrix of a Three-Phase Voltage Unbalance Factor. *IEEE Trans. Power Syst.* **2018**, *33*, 3192–3195. [CrossRef]
22. Quispe, E.C.; Santos, V.S.; López, I.D.; Gómez, J.R.; Viego, P.R. Theoretical Analysis of the Voltage Unbalance Factor to Characterize Unbalance Problems in Induction Motors. *Int. Rev. Electr. Eng.* **2021**, *16*, 8–16. [CrossRef]